Translational Oncology
www.transonc.com

Volume 10 Number 6 December 2017 pp. 911–916 911

MRI Texture Analysis Reflects Histopathology Parameters in Thyroid Cancer – A First Preliminary Study

Hans-Jonas Meyer*, Stefan Schob†, Anne Kathrin Höhn‡ and Alexey Surov*

*Department of Diagnostic and Interventional Radiology, University of Leipzig, Leipzig, Germany; †Department of Neuroradiology, University of Leipzig, Leipzig, Germany; ‡Department of Pathology, University of Leipzig, Leipzig, Germany

Abstract

OBJECT: Thyroid cancer represents the most frequent malignancy of the endocrine system with an increasing incidence worldwide. Novel imaging techniques are able to further characterize tumors and even predict histopathology features. Texture analysis is an emergent imaging technique to extract extensive data from an radiology images. The present study was therefore conducted to identify possible associations between texture analysis and histopathology parameters in thyroid cancer. *METHODS:* The radiological database was retrospectively reviewed for thyroid carcinoma. Overall, 13 patients (3 females, 23.1%) with a mean age of 61.6 years were identified. The MaZda program was used for texture analysis. The T1-precontrast and T2-weighted images were analyzed and overall 279 texture feature for each sequence was investigated. For every patient cell count, Ki67-index and p53 count were investigated. *RESULTS:* Several significant correlations between texture features and histopathology were identified. Regarding T1-weighted images, S(0;1)Sum Averg correlated the most with cell count ($r = 0.82$). An inverse correlations with S(5;0)AngScMom, S(5;0)DifVarnc S(5;0), DiffEntrp and GrNonZeros ($r = -0.69$, -0.66, -0.69 and -0.63, respectively) was also identified. For T2-weighted images, Variance with $r = 0.63$ was the highest coefficient, WavEnLL_S3 correlated inversely with cell count ($r = -0.57$). WavEnLL_S2 derived from T1-weighted images was the highest coefficient $r = -0.80$, S(0;5)SumVarnc was positively with $r = 0.74$. Regarding T2-weighted images WavEnHL_s-1 was inverse correlated with Ki67 index ($r = -0.77$). S(1;0)Correlat was with $r = 0.75$ the best correlation with Ki67 index. For T1-weighed images S(5;0)SumofSqs was the best with $r = 0.65$ with p53 count. For T2-weighted images S(1;−1)SumEntrp was the inverse correlation with $r = -0.72$, whereas S(0;4)AngScMom correlated positively with $r = 0.63$. *CONCLUSIONS:* MRI texture analysis derived from conventional sequences reflects histopathology features in thyroid cancer. This technique might be a novel noninvasive modality to further characterize thyroid cancer in clinical oncology.

Translational Oncology (2017) 10, 911–916

Introduction

Thyroid cancer represents the most frequent malignancy of the endocrine system with an increasing incidence worldwide [1]. Most thyroid malignancies are well-differentiated carcinomas, namely, papillary and follicular carcinoma [1,2]. Medullary and undifferentiated carcinomas are rarer and account for 5% and 2% of all thyroid cancers, respectively [1]. Patients with well-differentiated carcinomas have an excellent prognosis, whereas patients with undifferentiated carcinomas have a very poor prognosis [2]. Currently, several imaging modalities, especially ultrasound and magnetic resonance imaging (MRI), are used in clinical practice for detection of the primary tumor, measure the size and assess possible infiltration of adjacent structures [2,3]. Furthermore, novel imaging

Address all correspondence to: Hans-Jonas Meyer, MD, Department of Diagnostic and Interventional Radiology, University Leipzig, Liebigstraße 20, 04103 Leipzig, Germany.
E-mail: Hans-Jonas.Meyer@medizin.uni-leipzig.de
Received 6 August 2017; Accepted 14 September 2017

1936-5233/17
https://doi.org/10.1016/j.tranon.2017.09.003

techniques are able to further characterize tumors and even predict histopathology features [4,5]. For example, apparent diffusion coefficient (ADC) values derived from diffusion weighted imaging (DWI) were significantly different in differentiated and undifferentiated thyroid carcinomas [3]. Moreover, skewness, a parameter derived from ADC histogram, was statistically significant lower/higher between nodal positive and nodal negative thyroid carcinomas [6]. Recently, it has been shown that ADC parameters correlated with histopathologic parameters Ki67 and p53 in thyroid cancer [3,6].

Texture analysis is a novel imaging technique to extract extensive data from radiology images [4]. Thereby, acquired data can be categorized into several groups. First-order statistics include skewness, kurtosis, and entropy of the histogram [4,5]. Second-order statistics, which is widely known under "texture analysis", describe spatial relationships between voxels with similar gray levels within a lesion [4]. Typically used texture parameters are the Gray Level Co-occurrence Matrix (GLCM, the Gray Level Run-Length Matrix (GLRLM), and the Gray Tone Difference Matrix (GTDM) (Incoroonato). Finally, higher-order statistics imposes filter grids on an image to extract repetitive or non-repetitive patterns [4]. Presumably, tumor heterogeneity on the histopathology structure might be reflected by this imaging technique. However, there are only few studies directly correlating texture analysis with histopathology [7,8].

Regarding thyroid cancer, texture analysis was used in ultrasonographic studies to discriminate between benign and malignant nodules previously [9–11]. Furthermore, one study investigated texture features on ADC maps [12]. However, previously, no study investigated conventional MRI sequences with texture analysis in thyroid cancer.

Therefore, we conducted this study to elucidate possible associations between MRI texture analysis and histopathologic parameters in thyroid cancer.

Material and Methods

This retrospective study was approved by the local ethics committee. The radiological database was reviewed for thyroid carcinoma. In total, 20 patients were identified, but only 13 patients with histopathologically confirmed thyroid carcinoma had received proper MRI and were enrolled in this present study. The study sample consists of 3 females (23.1%) and 10 males with a mean age of 61.6 years (range, 41–91 years). The histopathologic diagnoses were papillary carcinoma (n = 4, 30.8%), follicular carcinoma (n = 4, 30.8%), and anaplastic carcinoma (n = 5, 38.4%).

MRI

MRI of the neck was performed for all patients using a 3 T device (Magnetom Skyra, Siemens, Erlangen, Germany). For this study, the following sequences were analyzed:

- axial T2-weighted (T2w) turbo spin echo (TSE) sequence (TR/TE: 4000/69, flip angle: 150°, slice thickness: 4 mm, acquisition matrix: 200 × 222, field of view: 100 mm);
- axial T1-weighted (T1w) turbo spin echo (TSE) sequence (TR/TE: 765/9.5, flip angle: 150°, slice thickness: 5 mm, acquisition matrix: 200 × 222, field of view: 100 mm).

All images were available in digital form and were analyzed by an experienced radiologist (HJM) without knowledge of the histopathological diagnosis on a PACS workstation (Centricity PACS, GE Medical Systems, Milwaukee, WI, USA). Figure 1 shows a representative case of the patient sample.

Texture Analysis

T1 precontrast weighted images as well as T2-weighted images were transformed into DICOM format and processed offline with the texture analysis software MaZda (version 4.7, available at http://www.eletel.p.lodz.pl/mazda/) [13,14]. A polygonal ROI was placed on the representative slide within the boundary of the tumor on the T1 precontrast sequence and the T2-weighted sequence. For each ROI, gray-level normalization was performed, using the limitation of dynamics to μ ± 3SD (μ gray level mean, SD standard deviation) to minimize the influence of contrast and brightness variation, as it was done previously for similar investigations [15]. The extracted features are as follows: gray-level histogram (mean, variance, skewness, kurtosis, percentiles (1, 10, 50, 90, 99%)), co-occurrence matrix (angular second moment, contrast, correlation, entropy, sum entropy, sum of squares, sum average, sum variance, inverse difference moment, difference entropy, difference variance (for four directions and five interpixel distances (offsets; n = 1 to 5)), run-length matrix (run-length non-uniformity, gray-level non-uniformity, long run emphasis, short run emphasis, fraction of image in runs)), absolute gradient (gradient mean, variance, skewness, kurtosis, non-zeros), autoregressive model (theta 1 to 4, sigma), and wavelet transform (energies of wavelet transform coefficients in sub-bands LL,LH,HL,HH). Altogether, 279 texture features were retrieved from T1-precontrast and T2-weighted images each.

Histopathology

All thyroid carcinomas were surgically resected and histopathologically analyzed. In every case, the proliferation index was estimated on Ki-67 antigen stained specimens using MIB-1 monoclonal antibody (DakoCytomation, Glostrup, Denmark). Furthermore, p53 index was estimated using monoclonal antibody p57, clone DO-7 (DakoCytomation). Two high-power fields (0.16 mm^2 per field, ×400) were analyzed. The area with the highest number of positive nuclei was selected. Additionally, cellular density was calculated for each tumor as average cell count per five high-power fields (×400) using ImageJ package 1.48v (National Institute of Health, Bethesda, MD, USA) as described previously [16]. All histopathological sections were analyzed using a research microscope Jenalumar equipped with a Diagnostic instruments camera 4.2 (Zeiss, Jena, Germany).

Statistical Analysis

Statistical analysis was performed using GraphPad Prism (GraphPad Software, La Jolla, CA, USA). Collected data were evaluated by means of descriptive statistics (absolute and relative frequencies). Spearman's correlation coefficient (p) was used to analyze associations between texture features and histopathologic parameters. Differences between the tumor entities were investigated by Mann–Whitney test. In all instances, P values <.05 were taken to indicate statistical significance.

Results

Several significant correlations were identified between texture analysis features and histopathology parameters, the nonsignificant correlations are not shown. Tables 1a, 1b, 1c displays the correlations of T1 texture features and Tables 2a, 2b, 2c the correlations of T2 texture features.

Cell Count

Regarding T1-weighted images, S(0;1)Sum Averg correlated the most with cell count (r = 0.82). There were also inverse correlations with S(5;0)AngScMom, S(5;0)DifVarnc S(5;0), DiffEntrp and GrNonZeros (r = −0.69, −0,66, −0,69 and −0.63, respectively).

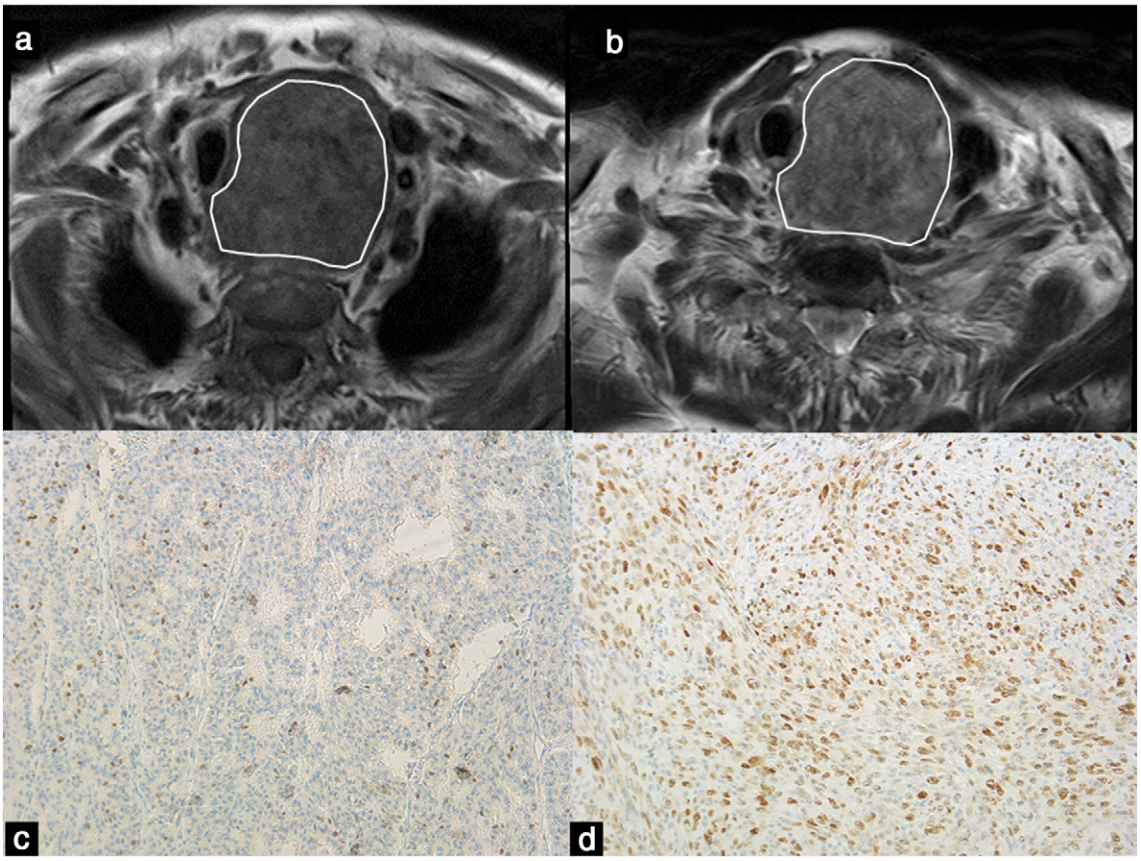

Figure 1. Imaging features and histopathological findings in a patient with anaplastic thyroid cancer. Placed ROIs within the lesion on T1 weighted and (a) T2-weighted images (b) of a large tumor in the left thyroid lobe. Histopathological findings of the tumors: MIB 1 staining (c) and p53 staining (d). Histopathological parameters are as follows: KI 67 index is 32%, p53 index is 66%, cell count is 1992, total nucleic area is 118,541 μm^2, and average nucleic area is 60 μm^2.

For T2-weighted images, variance with $r = 0.63$ was the highest coefficient, WavEnLL_S3 correlated inversely with $r = -0.57$.

Table 1a. Statistically Significant Correlations Between T1w Texture Analysis Features and Cell Count

Feature	*p*	*P*
S(0;1)Sum Averg	0.82	0.0005
S(0;1)InvDFMom	0.62	0.02
S(0;1)SumAverg	0.73	0.0045
S(1;1)SumVarnc	0.62	0.02
S(1;1)SumAverg	0.78	0.017
S(2;0)SumAverg	0.72	0.006
S(0;2)SumAverg	0.66	0.01
S(2;2)InvDfMom	0.61	0.03
S(2;2) SumAverg	0.65	0.02
S(3;0)SumAverg	0.68	0.01
S(0;3)SumAverg	0.57	0.04
S(3;3)Correlat	0.56	0.04
S(3;3) SumAverg	0.62	0.02
S(4;0)Contrast	0.65	0.01
S(4;0)InvDFMom	0.70	0.008
S(4;0) SumAverg	0.71	0.006
S(4;4) SumAverg	0.63	0.02
S(5;0)AngScMom	−0.69	0.01
S(5;0)Contrast	0.60	0.03
S(5,0)Correlat	0.60	0.03
S(5;0) SumAverg	0.66	0.01
S(5;0)DifVarnc	−0.69	0.009
S(5;0)DiffEntrp	−0.66	0.01
S(5;5) SumAverg	0.61	0.02
GrNonZeros	−0.63	0.02

Ki67

Some texture features derived from T1-weighted images correlated positively, others invers with Ki67. WavEnLL_S2 was the highest coefficient $r = -0.80$, S(0;5)SumVarnc was positively with $r = 0.74$. Regarding T2-weighted images also a wavelet transform feature (WavEnHL_s-1) was inverse correlated with Ki67 index ($r = -0.77$). S(1;0)Correlat was with $r = 0.75$ the highest coefficient.

P53

For T1-weighed images S(5;0)SumofSqs was the best with $r = 0.65$ with p53 count.

For T2-weighted images S(1;-1)SumEntrp was the inverse correlation with $r = -0.72$, whereas S(0;4) AngScMom correlated positively with $r = 0.63$.

Discussion

This is the first study to elucidate possible associations between MRI texture features derived from precontrast T1- and T2-weighted images and histopathology parameters in thyroid cancer to date. Notably, several second order statistics features like difference entropy, contrast, correlate and sum of squares correlate with the histopathology parameters. Interestingly, different features reflect different histopathology parameters.

Recently, texture analysis has become an emergent field in radiology with very promising results [4]. Especially in oncologic imaging, texture analysis features reflects several clinically relevant characteristics in several tumors [4]. Texture features show associations with molecular

Table 1b. Correlations Between T1w Texture Analysis Features and Ki67

Feature	*p*	*P*
MinNorm	0.60	0.03
Mean	0.63	0.02
Perc1%	0.65	0.02
Perc10%	0.56	0.04
Perc50%	0.62	0.02
S(1;1)DiffEntrp	−0.62	0.02
S(2;2)Contrast	−0.60	0.03
S(2;2)Correlat	0.63	0.02
S(2;2) InvDFMom	0.62	0.02
S(2;2) DiffEntrp	−0.70	0.008
S(0;3) DiffEntrp	−0.60	0.03
S(3;3)Contrast	−0.65	0.02
S(3;3) Correlat	0.64	0.02
S(3;3) InvDFMom	0.57	0.04
S(3;3)SumVarnc	0.60	0.03
S(3;3)DiffVarnc	−0.63	0.02
S(3;3) DiffEntrp	−0.64	0.02
S(4;0)Contrast	−0.57	0.04
S(4;0) DiffEntrp	−0.63	0.02
S(0,4)Contrast	−0.58	0.04
S(0;4)Correlat	0.63	0.02
S(0;4)SumVarnc	0.65	0.02
S(0;4) DiffVarnc	−0.63	0.02
S(0;4) DiffEntrp	−0.67	0.01
S(4;4)Contrast	−0.63	0.02
S(4;4)Correlat	0.66	0.01
S(4;4)InvDfMom	0.57	0.04
S(4;4)SumVarnc	0.65	0.02
S(4;4)SumEntrp	0.59	0.03
S(4;4)DiffEntrp	−0.69	0.009
S(5;0)Contrast	−0.57	0.04
S(0;5)Correlat	0.66	0.01
S(0;5)SumVarnc	0.74	0.004
WavEnLL_S2	−0.80	0.001
WavEnLL_S3	−0.62	0.02

markers, for example in low-grade gliomas, and can also be used as prognostic biomarkers [17]. Furthermore, they can predict the survival for glioblastoma patients [18,19].

Another promising aspect may be differentiation between different histological tumor types, which was previously not able with conventional imaging alone. In breast cancer, texture analysis could discriminate between lobular and ductal breast carcinomas [20]. In another recent study, it could discriminate between benign and malignant meningiomas [21].

Table 1c. Correlations Between T1w Texture Analysis Features and p53

Feature	*p*	*P*
S(1;0)SumVarnc	0.57	0.04
S(1;1)SumofSqs	0.57	0.04
S(1;-1)SumofSqs	0.60	0.03
S(2;2)SumofSqs	0.64	0.02
S(2;-2)SumofSqs	0.59	0.03
S(3;0)SumofSqs	0.57	0.04
S(0;3)SumofSqs	0.58	0.04
S(3;-3)SumofSqs	0.56	0.04
S(4;0)SumofSqs	0.59	0.03
S(4;4)SumofSqs	0.56	0.04
S(4;-4)SumofSqs	0.56	0.04
S(5;0)SumofSqs	0.65	0.01
S(0;5)SumofSqs	0.57	0.04
S(5;5)SumofSqs	0.57	0.04
WavEnLL_S3	0.56	0.04
WavEnLL_S4	0.61	0.02

Table 2a. Correlations Between T2 Texture Analysis Features and Cell Count

Feature	*p*	*P*
Variance	0.63	0.02
S(3;3)Entrp	0.57	0.04
S(4;0)Entrp	0.55	0.04
S(4;-4)Entrp	0.57	0.04
S(5;0)Entrp	0.62	0.03
S(5;-5)Entrp	0.55	0.04
WavEnLL_S3	−0.57	0.04

The principal hypothesis is that texture analysis is able to display tumor heterogeneity due to further characterizing of the image and to gain data, which can be used as biomarkers [4].

The tumor suppressor protein p53 plays a pivotal role in DNA damage response, cell differentiation, proliferation, and death [22]. In about 50% of cancers overall a mutation in the p53 gene can be found [23]. Furthermore, p53 is mutated in up to 80% of cases in undifferentiated thyroid cancers, less in differentiated thyroid cancers [22]. Clinically, p53 expression is associated with lymph node metastasis, tumor size in papillary thyroid cancers [23] and, therefore, provides important prognostic information. In a recent study, a positive correlation between ADC values and p53 expression could be identified in thyroid cancer [6]. Regarding texture analysis, Dang et al. established a prediction model with 7 texture features to predict the p53 expression with an accuracy of 81.3% in head and neck cancers [24]. The present study identified that sum square average features derived from T1 weighted images and entropy based features derived from T2-weighted images are associated with p53 count in thyroid cancer.

Table 2b. Correlations Between T2 Texture Analysis Features and Ki67

Feature	*p*	*P*
S(1;0)Contrast	−0.71	0.0061
S(1;0)Correlat	0.75	0.003
S(1;0)InvDifMoment	0.56	0.04
S(1;0)DifVarnc	−0.77	0.02
S(1;0)DifEntrp	−0.77	0.002
S(1;-1)InvDifMom	0.57	0.04
S(2;0)Contast	−0.75	0.003
S(2;0)Correlat	0.75	0.003
S(2;0)SumEntrp	0.65	0.01
S(2;0)DiffVarnc	−0.68	0.01
S(2;0)DiffEntrp	−0.75	0.003
S(2;-2)InvDifMom	0.64	0.02
S(3;0)Contrast	−0.71	0.006
S(3;0)Correlat	0.74	0.004
S(3;0)DiffVarnc	0.63	0.002
S(3;0)DiffEntrp	−0.67	0.02
S(3;0)DiffEntrp	−0.75	0.003
S(3;-3)InvDifMom	0.63	0.02
S(3;-3)Entrp	0.59	0.03
S(4;0)Contrast	−0.68	0.01
S(4;0)Correlat	0.74	0.004
S(4;0)SumEntrp	0.68	0.01
S(4;0)DiffVarnc	−0.67	0.01
S(4;0)DiffEntrp	−0.68	0.01
S(0;4)Entrp	0.59	0.03
S(5;0)Contrast	−0.63	0.02
S(5;0)Correlat	0.68	0.01
S(5;0)DiffVarnc	−0.63	0.02
S(5;0)DiffEntrp	−0.64	0.02
S(0;5)Entrp	0.57	0.04
Teta1	0.64	0.02
Sigma	−0.55	0.04
WavEnHL_s-1	−0.77	0.002
WavEnHL_s-2	−0.68	0.01

Table 2c. Correlations Between T2 Texture Analysis Features and p53

Feature	*p*	*P*
S(0;1)SumEntrp	−0.67	0.01
S(1;1)SumEntrp	−0.63	0.02
S(1;-1)SumEntrp	−0.72	0.006
S(0;3)Entrp	−0.57	0.04
S(3;3)AngScMom	0.56	0.04
S(0;4)AngScMom	0.63	0.02
GrSkewness	−0.71	0.006
GrKurtosis	−0.66	0.01

Ki67 is the clinically most used marker for proliferative activity in cancers [25]. For medullary thyroid carcinomas, it is a prognostic biomarker [25]. A lot of recent studies investigated possible associations between Ki67 index and MRI [26]. Regarding thyroid cancer, a negative correlation between ADC and Ki67 index was identified [3,6,27]. Various different texture features derived from T1w and T2w images showed associations with Ki67 index. This is in good agreement with a recent investigation, which identified significant correlation between T1w and T2w derived histogram based features and Ki67 index in cerebral lymphomas [28].

Regarding cellularity and MRI findings, it is well known that ADC values reflect cell density of tumors [29,30]. The explanation of that finding is that cells restrict the free diffusion and therefore with a higher cell density the ADC value is lowered [29,30]. This was recently investigated by two meta-analyses with moderate correlation coefficients of $r = -0.59$ and $r = -0.56$ [29,30]. Interestingly, the highest coefficient in this present study of "SumAverg" derived from T1w images is even higher than in the above-mentioned meta-analyses. Furthermore, this finding is similar with a recent study, investigating conventional MRI sequences in glioblastoma [31]. The authors identified a correlation coefficient of $r = 0.69$ with cell density derived from T1w postcontrast images. In addition, combining the different MRI sequences, namely T1w postcontrast, fluid attenuation recovery sequence and DWI (ADC), the correlation coefficient was higher: $r = 0.74$ [31]. These results underlined the fact that different MRI sequences reflect different microstructural features in tumors. However, there is still paucity of studies regarding thyroid cancer. Previously, one study investigated histogram derived parameters by ADC maps to analyze possible associations with histopathology in thyroid cancer [6]. In fact, ADC kurtosis correlated inversely with cellularity and 90th percentile ADC correlated inversely with Ki67 index [6].

Previously, MRI texture analysis was used on ADC maps to discriminate between benign and malignant thyroid nodules [12]. Using conventional ADC values only a sensitivity and specificity of 70% and 63%, respectively, was identified [12]. Use of texture analysis improved validity with a 92% sensitivity and 96% specificity, indicating the clinical benefit of this technique [12]. Mainly features from the co-occurrence matrix were important for this analysis [12]. This is comparable with the present study.

The identified findings showed high correlations between imaging and biological parameters. However, we think that texture analysis is not considered to replace histopathologic examinations but enable the possibility to gain information regarding tumor biology noninvasivley and repeatably. As an example, the tumor histopathology can change under therapy but for most cancers no further histopathology is acquired after the first diagnosis defining biopsy. Novel radiology analysis like histogram and texture analysis might be able to provide such crucial information in clinical routine. Another important aspect is that histopathology is nowadays more and more acquired with smaller biopsy samples and thus only displaying a small portion of the tumor. It is well known that larger tumors have different microenvironments [32] and therefore a biopsy might only provide information about a completely different tumor area than the main tumor.

This study has several limitations. Firstly, it is a retrospective analysis with the concordantly known bias. However, the radiologist doing the analysis was blinded for the histopathology results. Secondly, the patient sample is small. Thirdly, it is a known phenomenon in studies regarding texture analysis that the number of investigated imaging features largely extends the number of included patients with possible statistically problems. Therefore, a prospective study with a greater patient sample is needed to confirm our preliminary results.

Conclusions

MRI texture analysis derived from conventional sequences reflects different histopathological features in thyroid cancer. This technique might be a novel noninvasive modality to further characterize thyroid cancer in clinical oncology.

Funding Sources

This research did not receive any specific grant from funding agencies in the public, commercial, or not-for-profit sectors.

Conflicts of Interest

None.

Acknowledgements

None.

References

[1] Dal Maso L, Tavilla A, Pacini F, Serraino D, van Dijk BAC, Chirlaque MD, Capocaccia R, Larrañaga N, Colonna M, and Agius D, et al (2017). Survival of 86,690 patients with thyroid cancer: A population-based study in 29 European countries from EUROCARE-5. *Eur J Cancer* **77**(14), 140–152.

[2] Schmidbauer B, Menhart K, Hellwig D, and Grosse J (2017). Differentiated thyroid cancer-treatment: state of the art. *Int J Mol Sci* **18**(6) [pii: E1292].

[3] Schob S, Voigt P, Bure L, Meyer HJ, Wickenhauser C, Behrmann C, Höhn A, Kachel P, Dralle H, and Hoffmann KT, et al (2016). Diffusion-weighted imaging using a readout-segmented, multishot epi sequence at 3 T distinguishes between morphologically differentiated and undifferentiated subtypes of thyroid carcinoma—a preliminary study. *Transl Oncol* **9**(5), 403–410.

[4] Incoronato M, Aiello M, Infante T, Cavaliere C, Grimaldi AM, Mirabelli P, Monti S, and Salvatore M (2017). Radiogenomic analysis of oncological data: a technical survey. *Int J Mol Sci* **18**(4) [pii: E805].

[5] Just N (2014). Improving tumour heterogeneity MRI assessment with histograms. *Br J Cancer* **111**(12), 2205–2213.

[6] Schob S, Meyer HJ, Dieckow J, Pervinder B, Pazaitis N, Höhn AK, Garnov N, Horvath-Rizea D, Hoffmann KT, and Surov A (2017). Histogram analysis of diffusion weighted imaging at 3T is useful for prediction of lymphatic metastatic spread, proliferative activity, and cellularity in thyroid cancer. *Int J Mol Sci* **18**(4) [pii: E821].

[7] Wu X, Sikiö M, Pertovaara H, Järvenpää R, Eskola H, Dastidar P, and Kellokumpu-Lehtinen PL (2016). Differentiation of diffuse large B-cell lymphoma from follicular lymphoma using texture analysis on conventional mr images at 3.0 Tesla. *Acad Radiol* **23**(6), 696–703.

[8] Ko ES, Kim JH, Lim Y, Han BK, Cho EY, and Nam SJ (2016). Assessment of invasive breast cancer heterogeneity using whole-tumor magnetic resonance imagingtexture analysis: correlations with detailed pathological findings. *Medicine (Baltimore)* **95**(3), e2453.

[9] Kim SY, Lee E, Nam SJ, Kim EK, Moon HJ, Yoon JH, Han KH, and Kwak JY (2017). Ultrasound texture analysis: association with lymph node metastasis of papillary thyroid microcarcinoma. *PLoS One* **12**(4), e0176103.

[10] Bibicu D, Moraru L, and Biswas A (2013). Thyroid nodule recognition based on feature selection and pixel classification methods. *J Digit Imaging* **26**(1), 119–128.

[11] Chen S-J, Chang C-Y, Chang K-Y, Tzeng J-E, Chen Y-T, Lin C-W, Hsu W-C, and Wei C-K (2010). Classification of the thyroid nodules based on characteristic sonographic textural feature and correlated histopathology using hierarchical support vector machines. *Ultrasound Med Biol* **36**(12), 2018–2026.

[12] Brown AM, Nagala S, McLean MA, Lu Y, Scoffings D, Apte A, Gonen M, Stambuk HE, Shaha AR, and Tuttle RM, et al (2016). Multi-institutional validation of a novel textural analysis tool for preoperative stratification of suspected thyroid tumors on diffusion-weighted MRI. *Magn Reson Med* **75**(4), 1708–1716.

[13] Strzelecki M, Szczypinski P, Materka A, and Klepaczko A (2013). A software tool for automatic classification and segmentation of 2D/3D medical images. *Nucl Instrum Methods Phys Res A* **702**, 137–140.

[14] Szczypiński PM, Strzelecki M, Materka A, and Klepaczko A (2009). MaZda—a software package for image texture analysis. *Comput Methods Prog Biomed* **94**(1), 66–76.

[15] Fruehwald-Pallamar J, Czerny C, Holzer-Fruehwald L, Nemec SF, Mueller-Mang C, Weber M, and Mayerhoefer ME (2013). Texture-based and diffusion-weighted discrimination of parotid gland lesions on MR images at 3.0 Tesla. *NMR Biomed* **26**(11), 1372–1379.

[16] Surov A, Caysa H, Wienke A, Spielmann RP, and Fiedler E (2015). Correlation between different adc fractions, cell count, Ki-67, total nucleic areas and average nucleic areas in meningothelial meningiomas. *Anticancer Res* **35**(12), 6841–6846.

[17] Zhou H, Vallières M, Bai HX, Su C, Tang H, Oldridge D, Zhang Z, Xiao B, Liao W, and Tao Y, et al (2017). MRI features predict survival and molecular markers in diffuse lower-grade gliomas. *Neuro-Oncology* **19**(6), 862–870.

[18] Ingrisch M, Schneider MJ, Nörenberg D, Negrao de Figueiredo G, Maier-Hein K, Suchorska B, Schüller U, Albert N, Brückmann H, and Reiser M, et al (2017). Radiomic analysis reveals prognostic information in T1-weighted baseline magnetic resonance imaging in patients with glioblastoma. *Invest Radiol* **52**(6), 360–366.

[19] Kickingereder P, Burth S, Wick A, Götz M, Eidel O, Schlemmer HP, Maier-Hein KH, Wick W, Bendszus M, and Radbruch A, et al (2016). Radiomic profiling of glioblastoma: identifying an imaging predictor of patient survival with improved performance over established clinical and radiologic risk models. *Radiology* **280**(3), 880–889.

[20] Waugh SA, Purdie CA, Jordan LB, Vinnicombe S, Lerski RA, Martin P, and Thompson AM (2016). Magnetic resonance imaging texture analysis classification of primary breast cancer. *Eur Radiol* **26**(2), 322–330.

[21] Yan PF, Yan L, Hu TT, Xiao DD, Zhang Z, Zhao HY, and Feng J (2017). The potential value of preoperative mri texture and shape analysis in grading meningiomas: a preliminary investigation. *Transl Oncol* **10**(4), 570–577.

[22] Manzella L, Stella S, Pennisi MS, Tirrò E, Massimino M, Romano C, Puma A, Tavarelli M, and Vigneri P (2017). New insights in thyroid cancer and p53 family proteins. *Int J Mol Sci* **18**(6) [pii: E1325].

[23] Morita N, Ikeda Y, and Takami H (2008). Clinical significance of p53 protein expression in papillary thyroid carcinoma. *World J Surg* **32**(12), 2617–2622.

[24] Dang M, Lysack JT, Wu T, Matthews TW, Chandarana SP, Brockton NT, Bose P, Bansal G, Cheng H, and Mitchell JR, et al (2015). MRI texture analysis predicts p53 status in head and neck squamous cell carcinoma. *AJNR Am J Neuroradiol* **36**(1), 166–170.

[25] Tisell LE, Oden A, Muth A, Altiparmak G, Mölne J, Ahlman H, and Nilsson O (2003). The Ki67 index a prognostic marker in medullary thyroid carcinoma. *Br J Cancer* **89**(11), 2093–2097.

[26] Surov A, Meyer HJ, and Wiencke A (2017). Associations between apparent diffusion coefficient (ADC) and Ki 67 in different tumors: A meta-analysis. Part 1: ADCmean. *Oncotarget* **8**, 75434–75444. https://doi.org/10.18632/oncotarget.20406.

[27] Shi RY, Yao QY, Zhou QY, Lu Q, Suo ST, Chen J, Zheng WJ, Dai YM, Wu LM, and Xu JR (2017). Preliminary study of diffusion kurtosis imaging in thyroid nodules and its histopathologic correlation. *Eur Radiol*. https://doi.org/10.1007/s00330-017-4874-0 [Epub ahead of print].

[28] Meyer HJ, Schob S, Münch B, Frydrychowitz C, Garnov N, Quäschling U, Hoffmann KT, and Surov A (2017). *Histogram analysis of T1 weighted, T2 weighted, and postcontrast T1 weighted images in primary CNS lymphoma: correlations with histopathological findings—a preliminary study. Mol Imaging Biol.* https://doi.org/10.1007/s11307-017-1115-5 [Epub ahead of print].

[29] Surov A, Meyer HJ, and Wienke A (2017). *Correlation between minimum apparent diffusion coefficient (ADC_{min}) and tumor cellularity: a meta-analysis. Anticancer Res* **37**(7), 3807–3810.

[30] Surov A, Meyer HJ, and Wienke A (2017). *Correlation between apparent diffusion coefficient (ADC) and cellularity is different in several tumors: a meta-analysis. Oncotarget* **8**(35), 59492–59499.

[31] Chang PD, Malone HR, Bowden SG, Chow DS, Gill BJA, Ung TH, Samanamud J, Englander ZK, Sonabend AM, and Sheth SA, et al (2017). *A multiparametric model for mapping cellularity in glioblastoma using radiographically localized biopsies. AJNR Am J Neuroradiol* **38**(5), 890–898.

[32] Hanahan D and Weinberg RA (2011). *Hallmarks of cancer: the next generation. Cell* **144**(5), 646–674.